Vol. 5, No. 1, pp. 17-23, June 2006

INTERNATIONAL JOURNAL OF SAFETY
www.kosos.or.kr

Study on Coupled Resonance Frequencies and Acoustic Responses in a 3-D Acoustic Cavity with the Air-gap for Safer Driving Condition

Sang Wook Kang*

Department of Mechanical Systems Engineering, Hansung University, Seoul 136-792, Korea

(Received March 2, 2006; Accepted June 12, 2006)

Abstract : An investigation was carried out to determine the effect of the thickness of the air-gap installed between the roof metal sheet and the headliner on booming noise in passenger cars. In addition, a way of offering quieter driving condition to drivers and passengers was studied. It was found that a very thin air-gap corresponding to approximately 3/100 of the height of the passenger compartment causes noticeable change in the coupled resonance frequencies and acoustic responses. Furthermore, a guideline is proposed for determining an optimal air-gap thickness during design stage of the air-gap beneath the roof metal sheet for reducing booming noise.

Key words: air gap, booming noise, passenger car, resonant frequency

1. Introduction

In recent years, to obtain high power and effective fuel consumption of the engine, weight reduction of the passenger car has been necessary. This makes the vehicle body vibrate more heavily and causes interior noise to be generated more easily. This noise may influence the safety of a driver and passengers in high-speed driving condition.

Low frequency noise below 200Hz from engine- and wheel-vibrations often dominates the interior noise in vehicles. For the optimization of vehicle bodies, the interaction of body panels and the cavity modes has been studied[1-5]. On the other hand, the author has researched a way of using the air-gap between the headliner and the roof metal sheet for the optimization of the cavity modes[6, 7]. In the previous paper[6], the author developed the theoretical formulation to investigate the effect of the air-gap for the three-dimensional coupled model, based on the mode superposition method.

In the paper, the theoretical formulation is verified by comparing theoretical results with FEM results. Furthermore, the effect of the air-gap on coupled frequencies and acoustic response of the three-dimensional coupled model are investigated.

*Corresponding author: swkang@hansung.ac.kr

2. Coupled Frequencies and Acoustic Responses

2.1 Coupled Frequency

The acoustic-structural coupled equations governing the three-dimensional coupled model with the air-gap as shown in Fig. 1 are obtained as follows[6]:

$$(\Omega_n^{(1)^2} + j2d_n^{(1)}\Omega_n^{(1)}\omega - \omega^2)I_n^{(1)}A_n^{(1)} = \omega^2\rho c^2\sum_m B_m L_{nm}^{(1)} + j\omega\rho c^2 Q_e\phi_n^{(1)}(\mathbf{r}_e), \quad (1a)$$

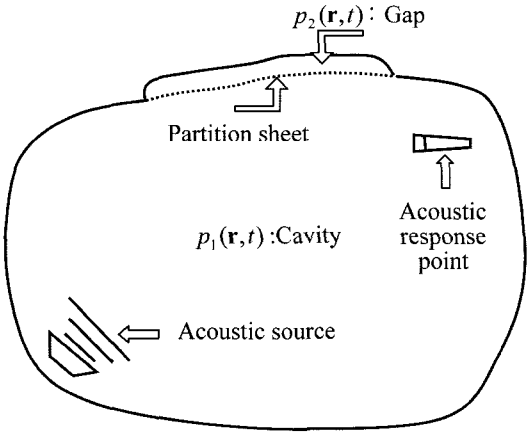

Fig. 1. Acoustic cavity with the air-gap and flexible partition sheet.

$$(\Omega_n^{(1)^2} + j2d_n^{(1)}\Omega_n^{(1)}\omega - \omega^2)I_l^{(2)}A_l^{(2)} = -\omega^2\rho c^2\sum_m B_m L_{lm}^{(2)}, \tag{1b}$$

$$(\lambda_m^2 + j2d_m\lambda_m\omega - \omega^2)\rho_s N_m B_m = \sum_n A_n^{(1)}L_{nm}^{(1)} - \sum_l A_l^{(2)}L_{lm}^{(2)}. \tag{1c}$$

Furthermore, Equations (1a-c) can be the single matrix equation

$$[-\omega^2\mathbf{M} + \omega\mathbf{C} + \mathbf{K}]\mathbf{X} = \mathbf{F} \tag{1d}$$

where

$$\mathbf{X} = \{\{A_n^{(1)}\}\ \{A_n^{(2)}\}\ \{B_m\}\}^T; \tag{2a}$$

$$\mathbf{F} = \left\{\left\{j\omega\rho c^2 Q_e \frac{\phi_n^{(1)}(\mathbf{r}_e)}{I_n^{(1)}}\right\}\ \mathbf{0}\ \mathbf{0}\right\}^T; \tag{2b}$$

$$\mathbf{M} = \begin{bmatrix} \mathbf{I} & \mathbf{0} & \mathbf{M}^{(13)} \\ \mathbf{0} & \mathbf{I} & \mathbf{M}^{(23)} \\ \mathbf{0} & \mathbf{0} & \mathbf{I} \end{bmatrix}; \quad \mathbf{K} = \begin{bmatrix} \mathbf{K}^{(11)} & \mathbf{0} & \mathbf{0} \\ \mathbf{0} & \mathbf{K}^{(22)} & \mathbf{0} \\ \mathbf{K}^{(31)} & \mathbf{K}^{(32)} & \mathbf{K}^{(33)} \end{bmatrix}; \tag{2c, 2d}$$

$$\mathbf{C} = \begin{bmatrix} \mathbf{C}^{(11)} & \mathbf{0} & \mathbf{0} \\ \mathbf{0} & \mathbf{C}^{(22)} & \mathbf{0} \\ \mathbf{0} & \mathbf{0} & \mathbf{C}^{(33)} \end{bmatrix} \tag{2e}$$

In the above: **X**, the displacement vector; **F**, the force vector; **I**, the identity matrix; the elements of $\mathbf{M}^{(13)}$ and $\mathbf{M}^{(23)}$ are given by

$$M_{nm}^{(13)} = \rho c^2 \frac{L_{nm}^{(1)}}{I_n^{(1)}},\ M_{lm}^{(23)} = -\rho c^2 \frac{L_{lm}^{(2)}}{I_l^{(2)}}; \tag{3,4}$$

the elements of the diagonal matrices $\mathbf{K}^{(11)}$, $\mathbf{K}^{(22)}$ and $\mathbf{K}^{(33)}$ are given by

$$K_{nm}^{(11)} = \Omega_n^{(1)^2},\ K_{ll}^{(22)} = \Omega_l^{(2)^2},\ K_{mm}^{(33)} = \lambda_m^2; \tag{5a-c}$$

the elements of $\mathbf{K}^{(31)}$ and $\mathbf{K}^{(32)}$ are given by

$$K_{mn}^{(31)} = -\frac{L_{nm}^{(1)}}{\rho_s N_m},\ \mathbf{K}_{lm}^{(32)} = \frac{L_{lm}^{(2)}}{\rho_s N_m}; \tag{6,7}$$

the elements of the diagonal matrices $\mathbf{C}^{(11)}$, $\mathbf{C}^{(22)}$ and $\mathbf{C}^{(33)}$ are given by

$$C_{nn}^{(11)} = 2j\zeta_n^{(1)}\Omega_n^{(1)},\ C_{ll}^{(22)} = 2j\zeta_l^{(2)}\Omega_l^{(2)},\ C_{mm}^{(33)} = 2j\zeta_m\lambda_m. \tag{8a-c}$$

In order to calculate the coupled frequencies of the coupled system, the modal damping constants and the external force are taken equal to zeros; i.e., **C=F=0**, which lead Equation (1d) to

$$[-\omega^2\mathbf{M}+\mathbf{K}]\mathbf{X} = \mathbf{0} \tag{9}$$

Then, the above equation can be rewritten in a conventional form associated with eigenvalue problems: i.e.,

$$\mathbf{DX}=\omega^2\mathbf{IX} \tag{10}$$

where **I** is the identity matrix of the order and **D** is the dynamic matrix:

$$\mathbf{D} = \mathbf{M}^{-1}\mathbf{K} \tag{12}$$

When obtaining the inverse of **M** to evaluate the dynamic matrix, we may be faced with the difficulty of numerical calculations involved in the inverse. However, no calculation of the inverse matrix is required because $\mathbf{M}^{-1}$ can be taken in an established close form:

$$\mathbf{M}^{-1} = \begin{bmatrix} \mathbf{I} & \mathbf{0} & -\mathbf{M}^{(13)} \\ \mathbf{0} & \mathbf{I} & -\mathbf{M}^{(23)} \\ \mathbf{0} & \mathbf{0} & \mathbf{I} \end{bmatrix} \tag{13}$$

It is noted that no inverse procedure is required to determine the coupled frequencies of the coupled system.

2.2 Acoustic Response

When an acoustic source is laid in the cavity, the acoustic response of the cavity is calculated from Equation (1d). In this case, the orders of the square matrices such as **M, C** and **K** are each $N_1+N_2+N_s$, which corresponds to the sum of the numbers of the acoustic and structural modes used in a coupled analysis. On the other hand, an alternative approach is introduced to reduce dimensions of Equation (1d).

Both the pressure responses in the cavity and gap and the displacement response in the partition are found by multiplying Equation (1d) by an inverse matrix:

$$\mathbf{X} = [-\omega^2\mathbf{M} + \omega\mathbf{C} + \mathbf{K}]^{-1}\mathbf{F} \equiv \mathbf{SM}^{-1}\mathbf{F} \tag{14}$$

where the system matrix **SM** is a square matrix whose order is equal to the sum of the mode numbers of the cavity, the gap and the partition used for the coupling analysis. If the unknown coefficient vector $\{A_n^{(1)}\}$ is obtained from **X**, the acoustic response in the cavity

can be found from [6]

$$p_1(\mathbf{r}, t) = \sum_{n=1}^{N!} A_n^{(1)} \phi_n^{(1)}(\mathbf{r}) e^{j\omega t} \tag{15}$$

Note that $\{A_t^{(2)}\}$ and $\{B_m\}$ can be also found from **X** in addition.

3. Verification and Discussion

3.1 Verification of the Theoretical Formulation

Consider a hexahedron cavity whose boundaries are assumed as rigid walls, except that the partition is a flexible wall. As may be seen in Fig. 2, the flexible partition is separated from the upper boundary of the cavity by a gap whose thickness is L_g and is fixed along the contact lines with the cavity. The partition has the following material properties and the thickness: Young's modulus, 2.5758 Gpa; material density, 305 kg/m^3; thickness, 5 mm.

Theoretical results are compared to the numerical ones that are obtained by performing the finite element analysis by means of the FEM solver (MSC/NASTRAN). In the theoretical and numerical analyses, all acoustic and structural modes below 300 Hz are participated, and the gap thickness L_g is given by 3 mm which corresponds to the gap ratio, 0.03. In Table 1 the theoretical coupled frequencies are compared with the numerical ones. The comparison shows good agreement, except that several high frequencies have some error. These errors may result from the small number of the meshes used for the FE modeling of the partition.

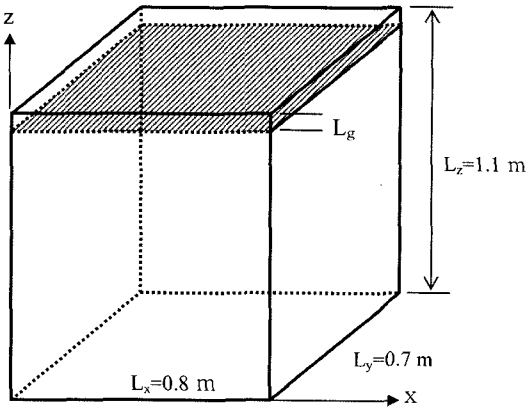

Fig. 2. Verification model with the air-gap beneath the upper boundary of the cavity; the dashed surface denotes the flexible partition sheet.

3.2 Coupled Frequencies

Understanding the one-dimensional results that has been introduced in the author's previous paper [7], it may be predicted that the first cavity frequency will be strongly influenced by the gap, at least when compared

Table 1. Comparison of the coupled frequencies between the theory and the FEM; the rigid acoustic (Helmholtz) modes of the cavity and gap are omitted; the parentheses below represent the corresponding mode shape numbers.

Coupled frequency (Hz)		Error (%)	Uncoupled frequency (Hz)		
FEM	Theory		Partition	Cavity	Gap
46.71	44.16	5.5	27.17 (1,1)	159.81 (0,0,1)	*214.94 (1,0,0)*
57.86	55.11	4.8	62.20 (2,1)	*214.94 (1,0,0)*	*245.64 (0,1,0)*
106.43	*106.43*	0.0	73.14 (1,2)	*245.64* (0,1,0)	
114.49	111.57	0.7	106.43 (2,2)		
142.62	141.54	0.8	120.76 (3,1)		
154.03	154.44	-0.3	149.94 (1,3)		
159.94	158.13	1.1	162.47 (3,2)		
176.25	172.45	2.2	180.81 (2,3)		
198.90	195.58	1.7	203.03 (4,1)		
214.94	*214.94*	*0.0*	232.80 (3,3)		
229.44	229.18	0.1	242.19 (4,2)		
242.19	*242.19*	*0.0*	257.71 (1,4)		
245.64	243.43	1.7	*286.17 (2,4)*		
247.63	*245.64*	*0.0*			
250.00	268.07	7.2			
286.17	*286.17*	*0.0*			
299.71	329.53	-9.9			
325.15	354.61	-9.1			

to the other cavity frequencies. This prediction may be valid because the first cavity mode has one nodal surface parallel to the partition; i.e., it is coupled well with the transverse vibration of the partition. However, unlike the one-dimensional model in which the coupling degree is not quantitatively established, in the three-dimensional model the coupling degree is represented by the coupling coefficients. Although the second or third cavity mode has no nodal surface to the partition, it may be changed thanks to non-zero coupling coefficients with the partition modes.

3.2.1 Mode uncoupling

It was clear that in the one-dimensional analysis the gap has an effect on the harmonic natural frequencies of the one-dimensional cavity as though the gap thickness is very thin compared to the cavity height. However, since many acoustic and structural modes are participated in the coupling of the real coupled system, it is required to grasp the trend of the change of the coupled frequencies by employing the coupling coefficients. In Table 2 are summarized the coupled frequencies obtained when the gap ratio is increased from 1% to 9% by 1%. It may be seen that some uncoupled frequencies remain constant as though the gap ratio is increased. This phenomenon may be explained by using two types of the coupling coefficients. The coupling coefficients between the cavity and the partition are called "cavity coupling coefficients," which are shown in Fig. 3a, and the coupling coefficient between the gap and the partition are called "gap coupling coefficients", which are shown in Fig. 3b.

In Table 2, the uncoupled frequencies of the partition, cavity and gap are marked by S1-S13, A1-A3 and G1-G2, respectively. When the gap thickness is increased, the uncoupled frequencies, S4, S11 and S13 remain constant, which results from the following facts:

1) The associated partition modes are uncoupled with all the cavity and gap modes in that the coupling coefficients become zeros as shown in Fig. 3: i.e., $L_{nm}^{(1)} = L_{lm}^{(2)} = 0$ for all n and m in the case of m = 4, 11, 13.

2) Theoretically, the uncoupling of the m-th partition mode is produced because the right side of Equation (1c) vanishes, which is satisfied in the case of $L_{nm}^{(1)}=0$ and $L_{lm}^{(2)}=0$ for all n and m. The partition modes corresponding to S4, S11 and S13 satisfy the above requirement.

Thus, it may be said that the coupled frequencies are sensitively dependent on the coupling coefficients in real coupled systems.

Next, the uncoupling of the cavity modes with the partition modes will be also theoretically explained by considering Equation (1a). The n-th cavity mode becomes uncoupled with the partition modes when all cavity coupling coefficients of Equation (1a) vanish; i.e., $L_{nm}^{(1)}=0$ for all m. However, as may be seen in Fig. 3a, any cavity mode inclusive of the Helmholtz mode doesn't satisfy the above requirement at all. Similarly, the l-th gap mode becomes uncoupled with the partition mode when all gap coupling coefficients of Equation (1b)

Table 2. Change in the coupled frequencies with increase in the gap ratio

	Uncoupled frequency	1 %	2 %	3 %	4 %	5 %	6 %	7 %	8 %	9 %
S1	27.41	31.87	39.99	44.51	47.45	49.52	51.07	52.27	53.23	54.01
S2	63.08	41.00	50.45	55.45	58.61	60.79	62.39	63.62	64.59	65.37
S3	73.99	109.66	109.66	109.66	109.66	109.66	108.95	107.24	105.40	103.50
S4	109.66	114.91	114.07	113.07	111.89	110.51	109.66	109.66	109.66	109.66
S5	122.52	145.28	144.28	142.95	141.31	139.47	137.57	135.75	134.11	132.69
S6	151.53	154.51	154.40	154.23	154.04	153.85	153.67	153.51	153.38	153.27
A1	154.54	162.83	163.70	164.35	164.84	165.24	165.55	165.82	166.04	166.23
S7	169.10	175.85	176.82	177.62	178.28	178.84	179.32	179.74	180.10	180.43
S8	187.29	198.53	198.64	198.74	198.84	198.93	199.02	199.10	199.18	199.26
S9	205.73	212.50	212.50	212.50	212.50	212.50	211.54	206.01	202.55	200.51
A2	212.50	242.86	242.86	241.05	231.69	220.00	212.50	212.50	212.50	212.50
G1	212.50	245.11	244.08	242.86	242.86	242.86	242.86	242.86	242.86	242.86
A3	242.86	245.64	245.54	245.45	245.37	245.29	245.22	245.15	245.09	245.03
G2	242.86	252.31	252.31	252.31	252.31	250.05	248.89	248.36	248.06	247.88
S10	246.73	295.98	295.98	270.33	253.83	252.31	252.31	252.31	252.31	252.31
S11	252.31	429.46	315.11	295.98	295.98	293.17	283.39	276.12	270.49	265.98
S12	260.32	464.25	367.70	328.72	307.09	295.98	295.98	295.98	295.98	295.98
S13	295.98	482.31	390.09	353.60	333.68	321.04	312.30	305.87	300.96	297.07

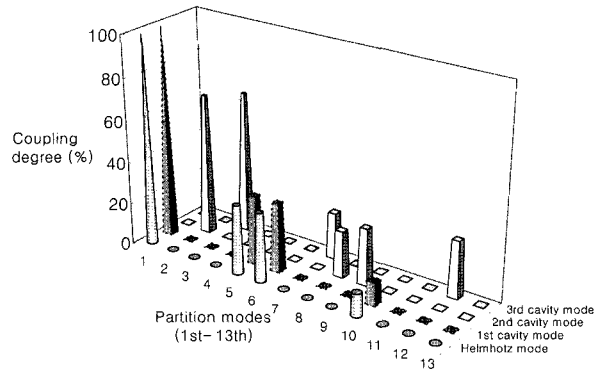

(a) Cavity coupling coefficients $L_{nm}^{(1)}$

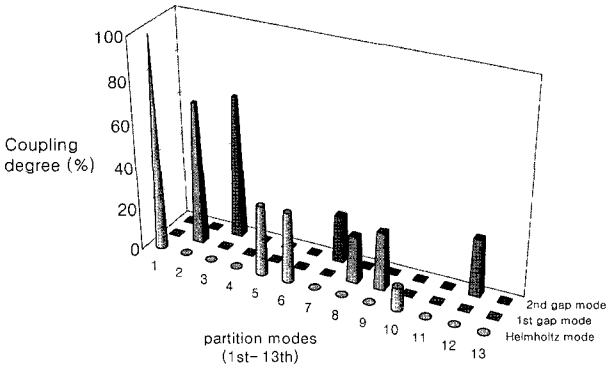

(b) Gap coupling coefficents, $L_{lm}^{(2)}$

Fig. 3. Coupling coefficients, $L_{nm}^{(1)}$ and $L_{lm}^{(2)}$ of the verification model; the Helmholtz modes denote the acoustic rigid modes of the cavity or air-gap.

vanish; i.e., $L_{lm}^{(2)}=0$ for all m. However, it may be confirmed from Fig. 3b that there is no the gap mode which satisfies the above requirement.

From the considerations on the uncoupling of the cavity and gap modes, it may be predicted that all the cavity and gap modes will be influenced by the partition modes. Nevertheless, as shown in Table 2, the uncoupled frequencies, 212.50 Hz and 242.80, keep constant values as though the gap ratio is increased. This theoretical discrepancy may be connected with the fact that the second and third uncoupled frequencies (A2 and A3) of the cavity are equal to the first and second ones (G1 and G2) of the gap, respectively: i.e., A2=G1 and A3=G2. In these cases, only one of the same uncoupled frequencies is changed but the other hold an invariable state when the gap ratio is increased.

3.2.2 Mode coupling

The transmission degree of the partition vibration to the cavity is closely related to the cavity coupling coefficients, $L_{nm}^{(1)}$. The vanishment of $L_{nm}^{(1)}$ means that the m-th partition mode makes no contribution to the coupling with the n-th cavity mode. In the gap coupling coefficients, the vanishment of $L_{lm}^{(2)}$ means that there is no contribution of the l-th gap mode to the m-th partition mode. Thus it may be said that the coupling of a cavity mode will be created even when only one of all cavity coupling coefficients becomes nonzero. Considering the circumstance that many coupling coefficients have non-zero values in Fig. 3, it may be said that the non-zero coefficients have a complicated effect on the coupled frequencies. This effect will be dealt with in the next paper in a global sense.

3.3 Acoustic Responses

It has been shown from the one-dimensional analysis of the previous paper [7] that the thickness of the air-gap has an important effect on the acoustic responses of the one-dimensional model. Similarly, an air-gap effect in the three-dimensional model is examined as the thickness of the air-gap varies. Here, acoustic responses inside the cavity are plotted as a function of the excitation frequency in the concerned frequency range, which is determined between 50 Hz and 400 Hz. The modal damping factors are approximately given in the way that the modal damping factors of the cavity, gap and partition modes are set to 0.02. Note that the damping factors of the partition modes are generally larger than the present value because the partition sheet is made from high damping materials.

Fig. 4 shows the trend of the change of the acoustic response as increasing the gap ratio when the partition material density is set to the present value, which corresponds to twice the density used in previous section. It may be seen that the gap begins to come into effect on the first cavity resonant peak only for "Gap ratio= 0.03", in which the damped frequency zone comes up close to the first cavity resonant peak. Until the gap ratio comes to 0.09, the peak shift phenomenon is progressed with increasing speed in company with the movement of the damped frequency zone in the direction of the low frequency region.

As may be shown in the acoustic response for "Gap ratio=0.05", it may be seen that the first resonant peak is a little decreased and simultaneously a small peak is created in the left side. This phenomenon is related to the initial stage that the first resonant peak starts to be split into two resonant peaks. As the gap ratio is increased more largely (See Fig. 4d-e), the split phenomenon is observed definitely by degrees.

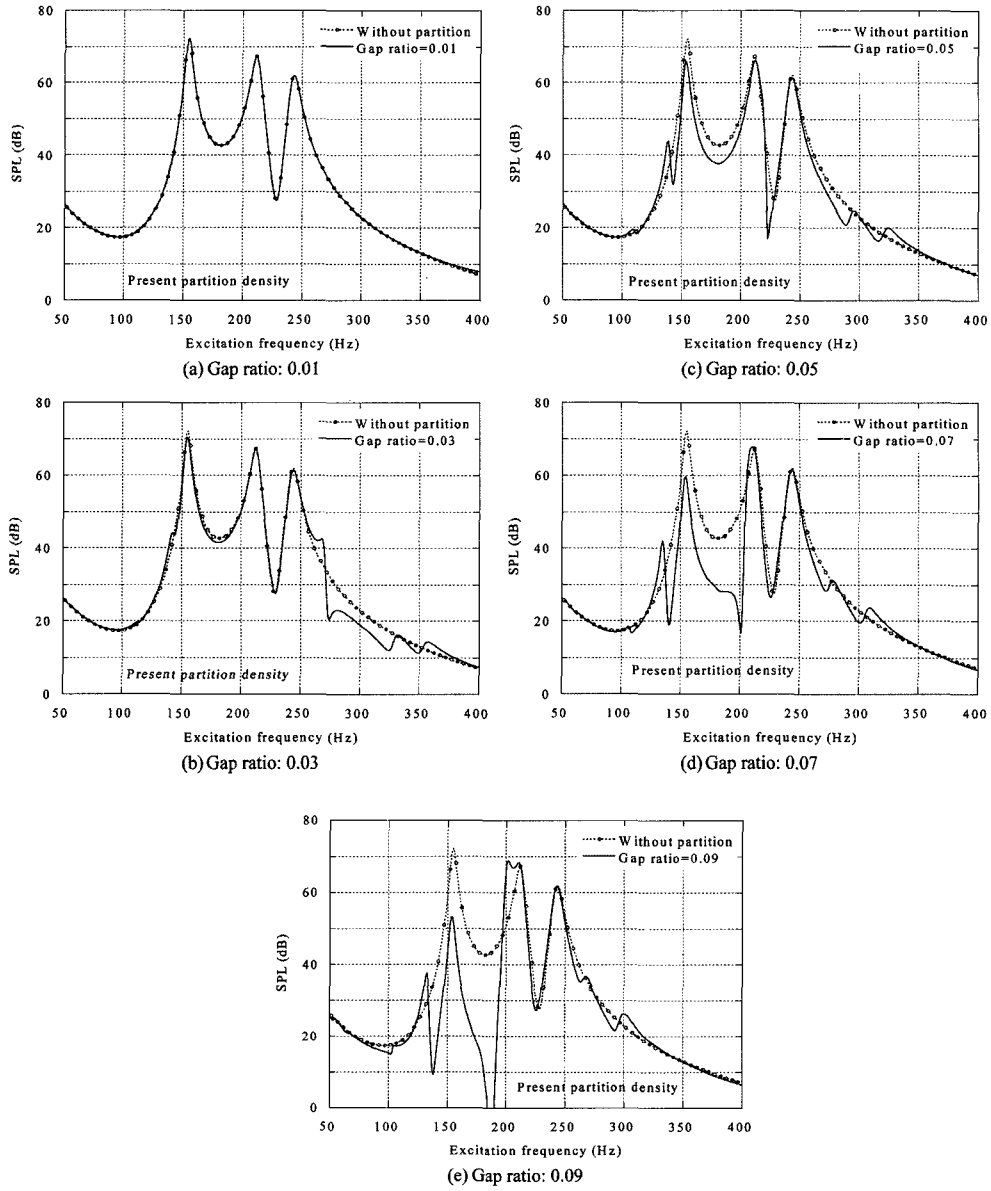

Fig. 4. Change in the acoustic responses with increased gap ratio with the present partition material density.

4. Conclusions

It is well known that the partition has a significant effect on the acoustic responses as well as on the coupled frequencies of the cavity thanks to the coupling with the gap. This is true even when the gap thickness is thin compared with the cavity dimensions and the partition density is low. The most dominant effect is to decrease the resonant peak controlled by the cavity mode that has more than one nodal surface parallel to the partition. As the gap thickness is increased, the damped frequency zone is moved from the high frequencies to the low ones. Thus, in a practical circumstance that the maximum value of the gap thickness is limited, the density may be considered as the main factor for moving the damped frequency zone close to a cavity resonant peak for the purpose of decreasing its level.

Unlike the one-dimensional analysis reported in the previous paper[7], the resonant peak of the up/down cavity mode has been split into several resonant peaks because many partition modes are coupled with the cavity mode. In addition, the damped frequency zone has no effect on the resonant peaks controlled by the cavity modes having no nodal surface parallel to the partition.

Acknowledgement

This research was financially supported by Korea

Sanhak Foundation in the year of 2004.

[1] J. A. Smith, R. C. Reid and A. F. Barnes, "Approach to Safety Control of Robot Manipulators", Journal of Hazardous Materials, Vol, 10, No. 5, pp. 44~50, 2001.

References

[1] K. K. Choi, "Design Sensitivity Analysis of Structure-induced Noise and Vibration," ASME Transactions, Journal of Vibration and Acoustics, Vol. 119 No. 2, pp. 173-179, 1997.

[2] E. H. Dowell, "Acoustoelasticity: General Theory, Acoustic Natural Modes and Forced Response to Sinusoidal Excitation, including comparisons with Experiments," Journal of Sound and Vibration, Vol. 52, No. 4, pp. 519-542, 1977.

[3] I. Hagiwara, and Z. D. Ma, "Sensitivity Calculation Method for Conducting Modal Frequency Response Analysis of Coupled Acoustic-structural Systems," JSME International Journal Series III, Vol. 35, No. 1, pp. 14-21, 1992.

[4] T. Osawa, and A. Iwama, "A Study of Vehicle Acoustic Control for Booming Noise Utilizing the Vibration Characteristics of Trunk Lid," SAE861410, pp. 187-192, 1986.

[5] J. A. Raff and R. D. Perry, "A Review of Vehicle Noise Studies Carried out at The Institute of Sound and Vibration Research with a Reference to Some Recent Research on Petrol Engine Noise," Journal of Sound and Vibration, Vol.28, No. 3, pp. 433-470, 1973.

[6] S. W. Kang, "Three dimensional formulation for interior acoustic field considering the airgap and the headliner," Hansung Journal, Vol. 29, pp. 1-11, 2005.

[7] S. W. Kang and J. M. Lee, "Sound Absorption Characteristics of Air-gap Systems in Enclosed Cavities," Journal of Sound and Vibration, Vol. 259, No. 1, pp. 209-218, 2003.